8th International Symposium on Magnetic Bearing
August 26-28, 2002, Mito, Japan

# A PRINCIPLE AND A DESIGN OF A CONSEQUENT-POLE BEARINGLESS MOTOR

**Tomohiro Takenaga, Yutaka Kubota, Akira Chiba**
Department of Electrical Engineering, Faculty of Science and Technology
Tokyo University of Science, 2641 Yamazaki, Noda, Chiba, Japan
**chiba@ee.noda.sut.ac.jp**

**Tadashi Fukao**
Department of Electrical Engineering, Faculty of Technology,
Musashi Institute of Technology Tamatsutumi, Setagaya, Tokyo, Japan

## ABSTRACT
In this paper, a consequent-pole bearingless motor is proposed. A rotor has buried permanent magnets, of which polarities are like. The radial force of a consequent-pole bearingless motor is generated by dc current. Thus, rotational angular position is not needed in a magnetic suspension controller. Radial force variations caused by a rotor rotation are minimized by improving arrangement of stator suspension conductors. A prototype bearingless motor and its controller are built. In experiment, principles of magnetic suspensions in the proposed consequent-pole bearingless drive are confirmed.

## INTRODUCTION
Recently, bearingless motors, that is an electro-magnetically integration of a magnetic bearing and a motor, have been developed in several countries. In permanent magnet bearingless motors, various types have been proposed. For example, surface mounted permanent magnet [1-3], inset permanent magnet [4], buried permanent magnet [5-6], interior permanent magnet, homopolar [7], hybrid [8] and etc. However, the most of these permanent magnet bearingless motors needs a rotor rotational angular position in a feedback magnetic suspension controller. If the field rotational position has a significant error, the magnetic suspension loop may not be stable. In homopolar and hybrid motors, a magnetic suspension controller does not need an exact angular position of magnetic field. These bearingless motors have axial flux flow, thus, suitable for more than 4-axis active magnetic suspension.

In this paper, a new bearingless motor is proposed. The proposed machine is originated from a consequent-pole permanent magnet motor. Radial force is generated by dc current like homopolar and hybrid PM motors, although the axial flux flow does not exist. High reluctance and trade off problems in permanent magnet bearingless motors are avoided. Rather thick permanent magnets are preferred for both torque and radial force generation. There is no trade off in a PM thickness and MMF requirements in suspension windings. In this paper, a previous paper [9] written in Japanese is briefly summarized and some new FEM and experimental results are included.

## PRINCIPLE OF CONSEQUENT-POLE MOTOR
Fig.1 shows a cross section of rotor and stator cores of a consequent-pole bearingless motor. Four permanent magnets, indicated by bold lines, are buried in a rotor iron. Polarities of the permanent magnets are unique. The permanent magnets are pre-magnetized in the same radial direction. All permanent magnets are polarised so that the outside and inside are N and S poles, respectively. Bold arrows represent flux flow generated by permanent magnets. The flux goes across the airgap, the stator tooth, the stator yoke, then, neighboring stator tooth, airgap, a rotor iron pole, and then returns to the permanent magnets. Thus, the iron poles between permanent magnets are consequently magnetized as S-pole, because the flux enters in the rotor iron pole. Thus, this motor is called as a consequent-pole motor [10]. This motor has totally 8 poles, i.e, four permanent magnet poles and four consequently magnetized iron poles.

Fig.2 shows flux flow with torque current in motor windings. Motor winding is arranged as 8-pole 3-phase windings, indicated by 8u, 8v, and 8w. In the figure, a rotor rotational angular position is 0deg. In this situation, torque is generated with zero u -phase current, positive v-phase current, and negative w-phase. In the flux plots, one can see that flux densities of stator teeth

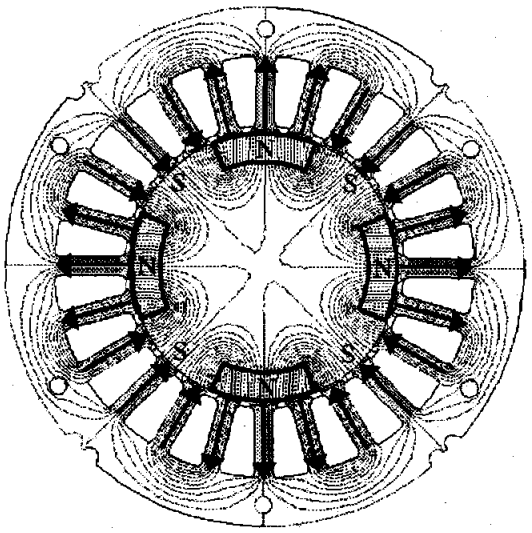

**FIGURE 1:** A cross section of rotor and stator cores, and rotor permanent magnets.

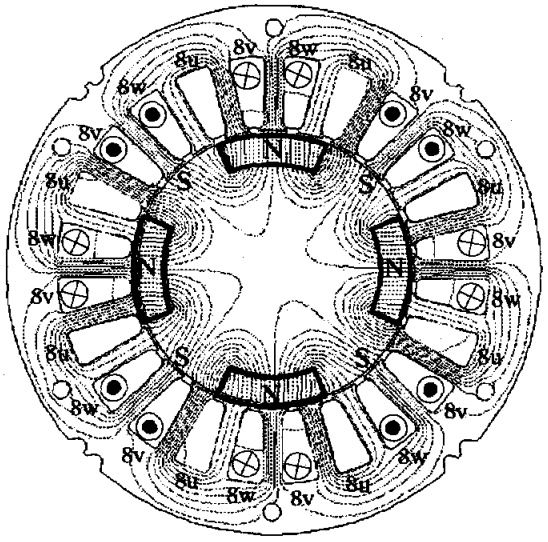

**FIGURE 2:** Flux plots with torque current in motor windings.

are unbalanced in comparison to the Fig.1, then, torque is generated in counter clockwise direction.

## PRINCIPLE OF RADIAL FORCE GENERATION

In a consequent-pole bearingless motor, a principle of radial force generation is different from conventional bearingless motors. Fig.3 shows a principle of radial force generation at a rotor rotational angular position $\phi_m$ = 0deg. Suspension conductors $N_x$ and $N_y$ are arranged in 2-pole two-phase windings. The $N_x$ indicates

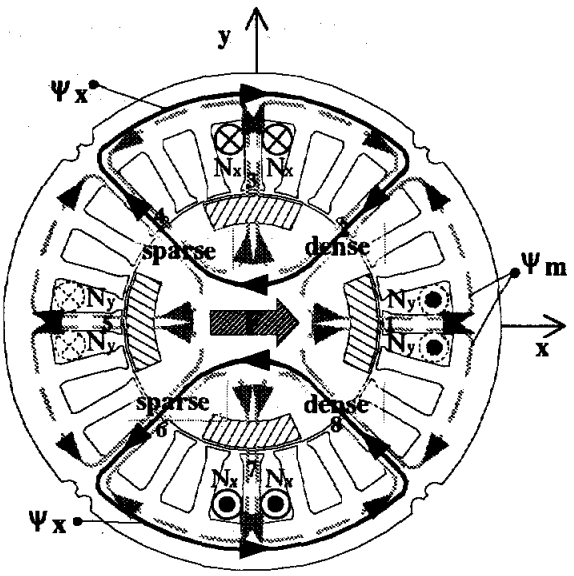


**FIGURE 3:** Radial force generation at $\phi_m$ = 0deg.

suspension conductors in order to generate radial force in the x-axis direction. The winding $N_y$ is for the y-direction radial force. Then, eight loops $\Psi_m$ indicated by broken line show representitive permanent magnet flux paths. Solid line loops $\Psi_x$ show suspension flux paths generated by positive current in $N_x$ suspension winding. Radial force is generated by an interaction between PM and suspension fluxes. In the airgaps 2 and 8, the flux densities are increased as indicated by "dense". However, in the airgaps 4 and 6, the flux densities are decreased, as indicated by "sparse". Therefore, radial force is generated in the x-direction. If negative direction current is supplied in $N_x$-winding, then, negative radial force is generated. The y-axis radial force is generated by $N_y$-winding current.

Note that suspension flux paths $\Psi_x$ does not go across permanent magnets. In the rotor, it goes through rotor iron poles. Thus, reluctance in the suspension flux loop is low. It is obvious that low MMF is needed in radial force generation.

Fig.4 shows a principle of radial force generation at a rotor rotational angular position $\phi_m$ = 45deg. Corresponding to the rotor position, permanent magnet flux paths $\Psi_m$ are rotated by 45deg. The suspension fluxes $\Psi_x$ go through iron rotor poles because the reluctance is low. The flux densities in the airgaps 1 and 5 are increased and decreased, respectively. Radial force is generated in the x-axis direction. Note that the direction of radial force is still despite of a rotor rotation. One may notice that the principles of radial force generation are similar to homopolar and hybrid type bearingless motors.

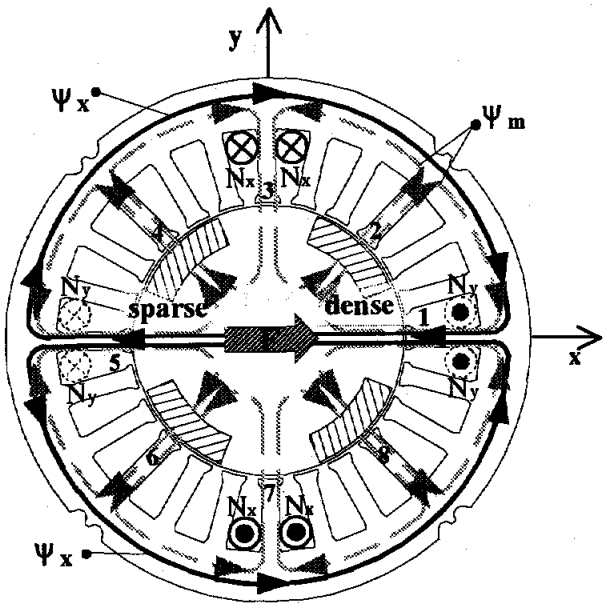


FIGURE 4: Radial force generation at $\phi_m$ = 45deg.

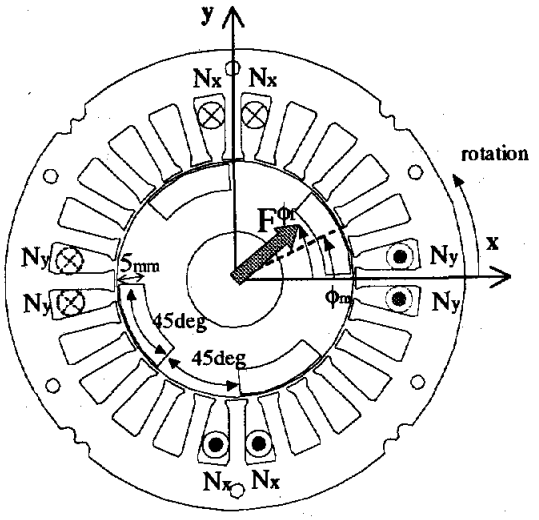


Rotor diameter : 49mm
Stack length: 50mm
Gap length : 0.5mm

FIGURE 5: FEM analysis model.

## RADIAL FORCE VARIATION

Fig.5 shows a FEM analysis model. In the analysis, only the dc current is supplied in $N_x$-winding. Then, radial force is supposed to be generated in the x-axis direction. The angular position $\phi_m$ is a rotor rotational angular position, the $\phi_f$ is an angular coordinate fixed to the x- and y- axes. Suspension conductors occupy two continuous stator slots with four series winding in one slot. Under this condition, a series of FEM analysis is carried out with a rotor rotation in a step of 5deg from 0deg up to 90deg.

Figs.6 (a) and (b) shows a result of a series of FEM analysis at 3A in the $N_x$-winding. Fig. (a) shows x- and y-axis radial forces $F_x$ and $F_y$. The horizontal axis is a rotor rotational angular position $\phi_m$. It is seen that $F_x$ is almost constant, however, $F_y$ is not always zero. Ideally, $F_y$ should be zero at any $\phi_m$. In the analysis, the $F_y$ is zero only at $\phi_m$ = 0,45 and 90deg.

Fig.6 (b) shows the radial force direction $\phi_f$. The $\phi_f$ is given by

$$\phi_f = \tan^{-1}\left(\frac{F_y}{F_x}\right) \qquad (1)$$

The largest value of $\phi_f$ is about 22.8deg at $\phi_m$ = 22.5deg and 67.5deg. This value of $\phi_f$ is not very acceptable in stable suspension positioning. In experimental view, $\phi_f$ should be less than 5deg.

Figs.7 (a), (b) and (c) show flux plots obtained from FEM analysis at $\phi_m$ = 0deg, 45deg and 22.5deg. The permanent magnets are assumed to be the air to see flux path exciting $N_x$-winding. Bold arrows represent flux flow caused by permanent magnets. Thin arrows represent suspension flux flow.

In Figs. (a) and (b), the flux flow is symmetrical with respect to the x-axis. Thus, radial force is generated only in the x-axis direction. In Fig. (c), the flux plot of suspension and PM is not symmetrical to the x-axis. The forces $F_1$ and $F_2$ are generated at the rotor iron poles. The resulted radial force F is not aligned to the x-axis. Consequently, the resultant force F is inclined with respect to the x-axis.

## SUSPENSION CONDUCTOR ARRENGEMENT

Fig.8 (a) and (b) shows alternative arrangements of stator suspension conductors. In Fig. (a), the suspension conductors are distributed in 4 continuous slots. In Fig. (b), the suspension conductors are arranged as 3- phase windings. The $N_u$, $N_v$ and $N_w$ are u-, v- and w-phase windings.

The winding currents $i_u$, $i_v$ and $i_w$ are determined by the transformation from 2-phase to 3-phase matrix as,

$$\begin{bmatrix} i_u \\ i_v \\ i_w \end{bmatrix} = \sqrt{\frac{2}{3}} \begin{bmatrix} 1 & 0 \\ -\frac{1}{2} & \frac{\sqrt{3}}{2} \\ -\frac{1}{2} & -\frac{\sqrt{3}}{2} \end{bmatrix} \begin{bmatrix} i_x \\ i_y \end{bmatrix} \qquad (2)$$

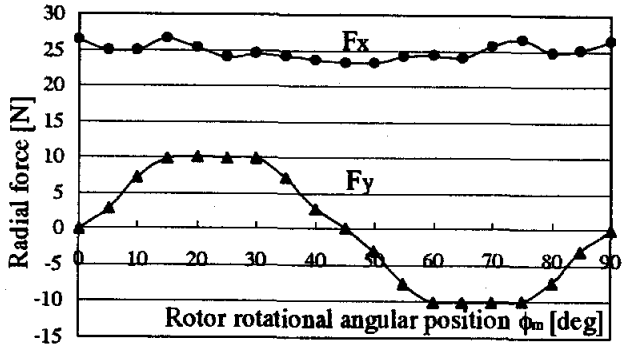


(a) Radial forces in two-perpendicular axis.

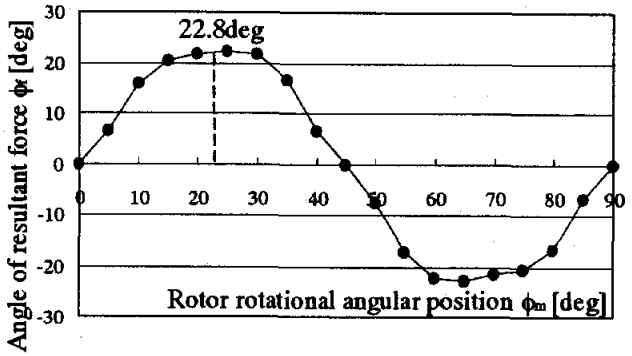


(b) Angular position of radial force direction.

**FIGURE 6:** Result of analysis.

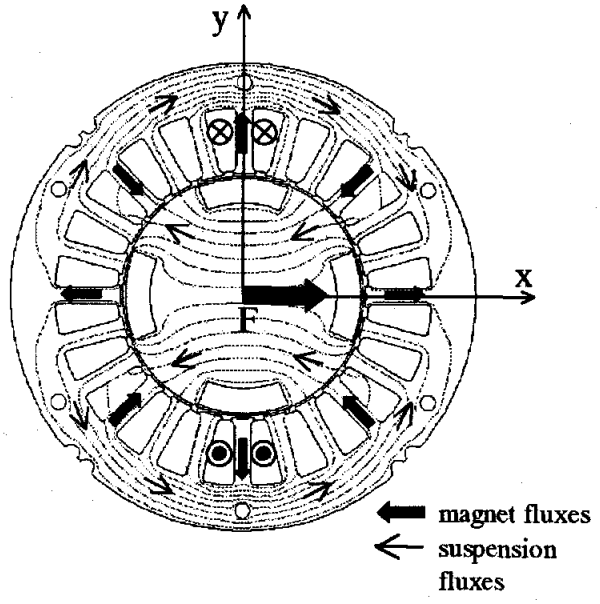


(a) Flux flow at $\phi_m$ = 0deg

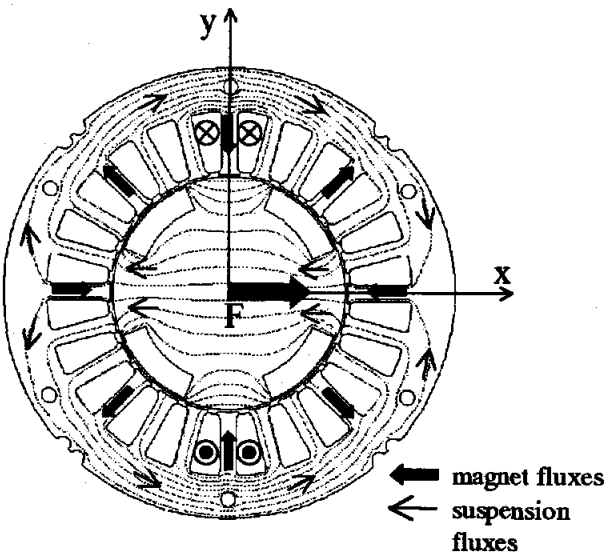


(b) Flux flow at $\phi_m$ = 45deg

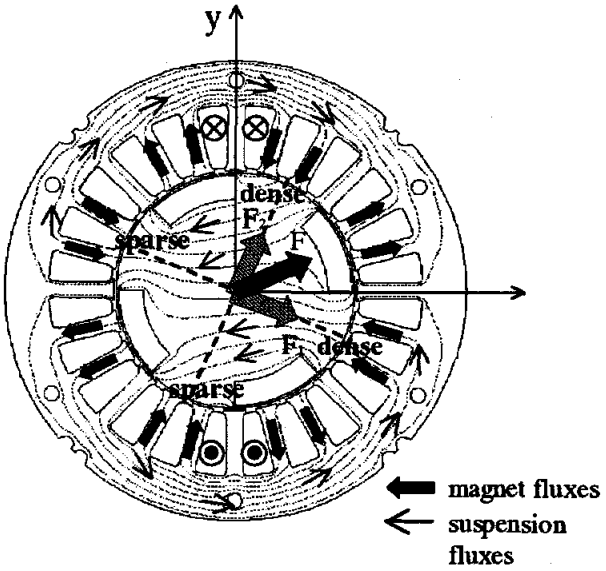


(c) Flux flow at $\phi_m$ = 22.5deg

**FIGURE 7:** Flux flow at various rotor positions.

Suspension conductor arrangements in 2-slot, 4-slot and three-phase conductor arrangements are hereafter referred as windings A, B and C, respectively.

Fig. 9 shows the direction of radial force for three conductor arrangements. The largest value of $\phi_r$ is 13.0deg and 3.3deg in winding B(4 slots) and C(3-phase), respectively. Significant reduction in radial force variations are realized by three-phase winding arrangement. Experiences tell us that the radial force variations within several degrees are acceptable.

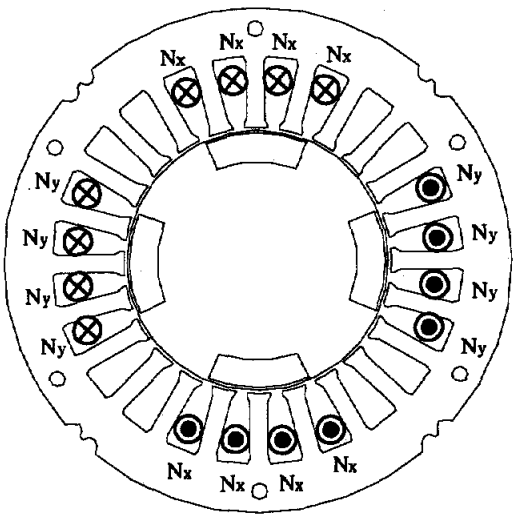


(a) Suspension conductor arrangement B.

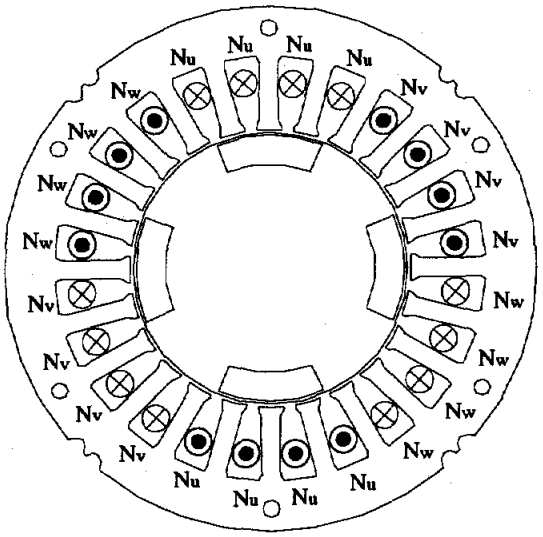


(b) Suspension conductor arrangement C.

**FIGURE 8:** Suspension conductor arrangements.

## EXPERIMENTAL RESULTS

Fig.10 shows a picture of a rotor in a prototype machine. All permanent magnets, polarised as shown in figure, are inserted into a laminated silicon steel stack. There are four permanent magnets, with a thickness of 5mm and an axial length of 50mm. Fig. 11 shows a test machine. The front machine is a consequent-pole bearingless motor, of which shaft is connected to a torque meter. The torque meter is connected to an induction generator.

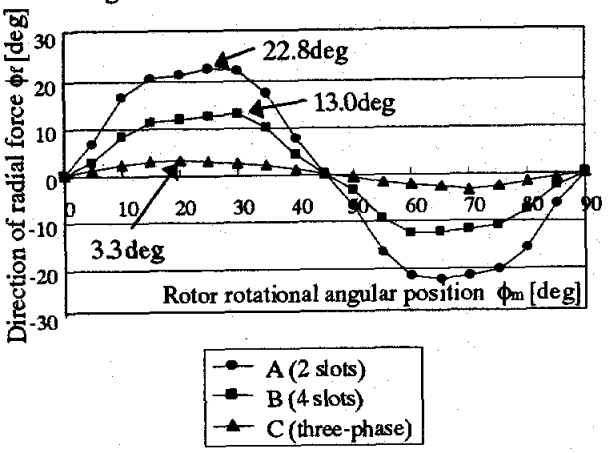


**FIGURE 9:** Radial force direction and conductor arrangements.

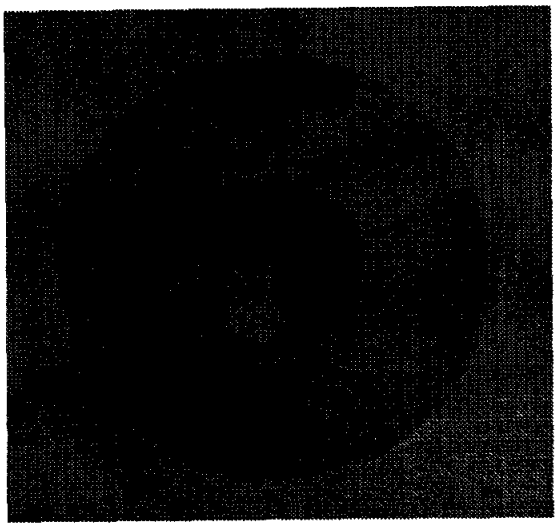

**FIGURE 10:** A rotor of a test machine.

In experiment, a reference value of $F_y^*$ is measured with a rotor rotation in a step of 15deg from -45deg to 45deg. The $F_y^*$ is the reference value of radial force in the y-axis magnetic suspension loop. The value of $F_y^*$ is voltage automatically developed in a PID controller. Magnetic suspension feedback loops are constructed. Shaft displacements are detected by displacement sensors. PID controllers generate radial force references.

Fig.12 shows the results of the experiment. From this experiment, it is clear that the radial force reference $F_y^*$ is generated almost at constant value to support a shaft weight. It is shown that radial force is not depending on a rotor rotational angular position.

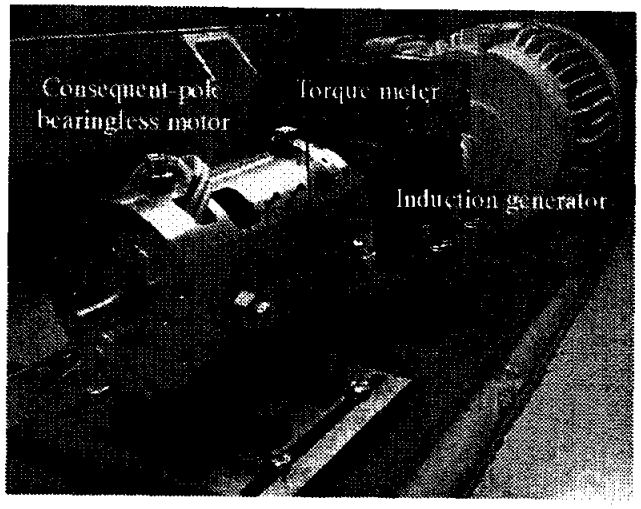


**FIGURE 11:** A test machine.

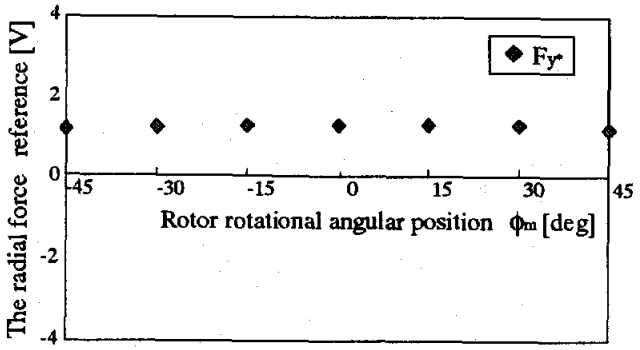


**FIGURE 12:** The radial force reference with respect to $\phi_m$.

## CONCLUSION

A principle and a design of a consequent-pole bearingless motor is proposed. In the analysis, it is shown that the radial force variations caused by a rotor rotation is minimized by proper conductor arrangement in suspension winding. In experiment, a principle is confirmed.

## REFERENCE

[1] Kousuke Oguri, Masaya Watada, Susumu Torii, Daiki Ebihara, "Design Optimization of Magnetic Bearing Composed of Permanent Magnets for the Bearing-Less Motor", International Symposium on Magnetic Bearings, August 23-25, 2000, ETH Zurich pp. 365-370

[2] Masahide Ooshima, Satoru Miyazawa, Akira Chiba, Fukuzo Nakamura, Tadashi Fukao, "Performance Evaluation and Test Results of a 11,000r/m, 4kW Surface-Mounted Permanent Magnet-Type Bearingless Motor", ISMB, August 23-25, 2000, ETH Zurich pp. 377-382.

[3] Barret Steele, Lyndon Stephens, "A Test Rig for Measuring Force and Torque Production in a Lorenz, Slotless Self Bearing Motor", ISMB, August 23-25, 2000, ETH Zurich pp. 407-412

[4] Kohei Inagaki, Akira Chiba, M.A.Rahman, Tadashi Fukao, "Performance Characteristics of Inset-Type Permanent Magnet Bearingless Motor Drives", PESWM, 23-27 January 2000 Singapore.

[5] Masahide Ooshima, Satoru Miyazawa, Yusuke Shima, Akira Chiba, Fukuzo Nakamura, Tadashi Fukao, "Increase in Radial Force of A Bearingless Motor with Buried Permanent Magnet-Type Rotor", Proceedings of the Fourth International conference on MOVIC, vol.3, pp. 1077-1082, 1998.

[6] Noriaki Fujie, Rintarou Yoshimatsu, Akira Chiba, Masahide Ooshima, M.A.Rahman, and Tadashi Fukao, "A Decoupling control Method of Buried Permanent Magnet Bearingless Motors considering Magnetic Saturation", IPEC-Tokyo2000, S-10-6pp. 395-400.

[7] Osamu Ichikawa, Akira Chiba, Tadashi Fukao, "Principles and Structures of Homopolar Type Bearingless Motors", IPEC-Tokyo 2000 pp. 401-406.

[8] Seung-Jong Kim, Tatsunori Shimonishi, Hideki Kaneboko, Yohji Okada, "Design of a Hybrid-Type Short-Span Self-Bearing Motor" ISMB, August 23-25, 2000, ETH Zurich pp. 359-364.

[9] Yutaka Kubota, Tomohiro Takenaga, Akira Chiba, "Proposed of Consequent-Pole Type Bearingless Motors" IEEJ, SPC-01-102 IEA-01-45, in Ashikaga Oct 2001(written in Japanese).

[10] J.R. Hendershot Jr, T.J.E Miller "Design of Brushless Permanent-Magnet Motors" Oxford Magna Physics 1994.